ANALYSIS OF EARDRUM PATHOLOGIES USING THE FINITE ELEMENT METHOD

FERNANDA GENTIL[*,†,§], CAROLINA GARBE[*,¶], MARCO PARENTE[*,‖], PEDRO MARTINS[*,**], ANTÓNIO FERREIRA[*,††,‖‖], RENATO NATAL JORGE[*,‡‡], CARLA SANTOS[*,§§] and JOÃO PAÇO[‡,¶¶]

[*]*IDMEC, Faculdade de Engenharia da Universidade do Porto, Portugal*

[†]*Clínica ORL-Dr. Eurico Almeida, Widex, ESTSP*

[‡]*Hospital CUF, Faculdade de Medicina da Universidade de Lisboa, Portugal*

[§]*fernanda.fgnanda@gmail.com*

[¶]*garbe@fe.up.pt*

[‖]*mparente@fe.up.pt*

[**]*palsm@fe.up.pt*

[††]*ferreira@fe.up.pt*

[‡‡]*rnatal@fe.up.pt*

[§§]*fsantos.carla@gmail.com*

[¶¶]*Joao.Paco@jmellosaude.pt*

[††] Corresponding author.

[‖‖] Department of Mathematics, Faculty of Science, King Abdulaziz University, Saudi Arabia.

This work investigates the effect of eardrum perforations and myringosclerosis in the mechanical behavior of the tympano-ossicular chain. A 3D model for the tympano-ossicular chain was created and different numerical simulations were made, using the finite element method. For the eardrum perforations, three different calibers of perforated eardrums were simulated. For the micro perforation (0.6 mm of diameter) no differences were observed between the perforated and normal eardrum. For the numerical simulation of the eardrum with the largest perforation caliber, small displacements were obtained in the stapes footplate, when compared with the model representative of normal ossicular-chain, at low frequencies, which is related with major hearing loss in this frequency range. For the numerical simulations of myringosclerosis, the larger differences in the displacement field between the normal and modified model were obtained in the umbo. When observing the results in the stapes footplate, there were no significant differences between the two models, which is in accordance to the clinical data. When simulating an eardrum perforation along with myringosclerosis, there is a decrease in the displacements, both from the umbo and the central part of the stapes footplate, often associated with a pronounced hearing loss. It could be concluded that the reduced displacement of the stapes footplate may be related to a greater hearing loss.

Keywords: Biomechanics; eardrum; perforation; myringosclerosis; finite element method.

1. Introduction

The function of the human auditory system is, essentially, to transmit the sounds from outside, transforming them into electrical impulses to obtain auditory sensations that are the basis for communication among humans. The ear is divided into three parts: external, middle and inner.

The eardrum separates the external ear from the middle ear, which is inserted into the tympanic cavity and contains the ear ossicles (malleus, incus and stapes), attached to the cavity by ligaments, muscles and their tendons. A branch of the facial nerve, the chorda tympani, crosses this box.

Hearing is one of the most important senses and is essential in communication. The information received through the ears is fundamental in language acquisition and the human ability to speak. Any intervention aimed at alleviating hearing difficulties, are of the utmost importance. The stapes footplate comes into contact with the oval window and the mechanical energy is converted into hydraulic energy at the level of the inner ear and, in turn, into electrical energy, communicating any information to the cerebral cortex, via the auditory nerve. The eardrum is associated with various pathologies, being the most common the eardrum perforations and myringosclerosis,[1] Fig. 1.

The most common causes of perforations are by trauma with objects, pressure differentials, barotrauma, lightning blasts, blast waves from gunshots, fireworks and other loud noises, Eustachian tube malfunction or sequelae of ear infections.[2] Perforation causes sudden ear pain, sometimes with bleeding from the ear, hearing loss or noise in the ear. Most of these perforations heal spontaneously, by medication, or through surgical procedure (tympanoplasty).[3]

The myringosclerosis consists of the calcification of various areas of the eardrum, making it more rigid, showing a white card configuration, of greater or lesser extent, occurring most often after perforations. It is known that the perforations are usually associated with hearing losses greater than those of simple myringosclerosis.[4]

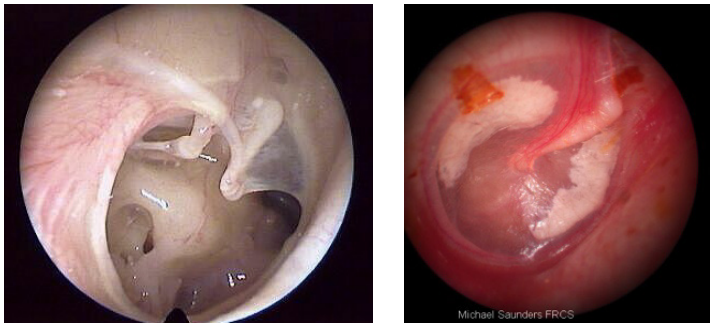

(a) (b)

Fig. 1. (Color online) (a) Eardrum perforation; (b) eardrum with myringosclerosis (white card configuration).

Patients with a ruptured eardrum may be at an increased risk of an ear infection, because the opening in the membrane allows bacteria to enter the middle ear and cause infection. The majority of small plaques of myringosclerosis do not cause any hearing loss. Some produce a very slight 1 dB or 2 dB loss in some of the frequencies. The myringosclerotic plaques can, however, be heavily calcified or ossified, impairing movements of the eardrum.[2] Histologically, these plaques reveal an increase in collagen and fibrous fibers with hyaline degeneration within the lamina propria of the pars tensa of the eardrum. This condition can often be found in children with secretory otitis who have undergone grommet insertion.

Some studies about eardrum pathologies in animals and humans have been developed and published.[5–11] Several publications compare their results with experimental and computational results of other authors. One study of Bigelow *et al.*[5] refers the effect of tympanic membrane perforation size on umbo velocity in the rat,[5] that reveal a systematic loss in low frequency velocity as perforation size increase. Other study of Gan *et al.*[6] predict the effect of the perforations on sound transmission through the middle ear, using a finite element model, and concludes that tympanic membrane perforation mainly affect the middle ear transfer function at low frequencies. Other experimental studies[8–11] were made studying the measurements of acoustic transmission in tympanic membrane perforated and conclude that perforations cause frequency-dependent loss, that is largest at low frequencies and increases as perforation size increases.

The insertion of a ventilation tube after myringotomy or other types of eardrum perforations lead to an increase in the prevalence of myringosclerosis. These complications are considered to be the most common of the middle ear, hence the need to establish a connection between the two pathologies. This work establishes in quantitative and qualitative ways the higher impact on hearing associated with perforations when compared to myringosclerosis. The simulations show that when considering the same affected area in the eardrum, the perforations induce a higher hearing impairment.

The objective of this work is to simulate eardrum perforations with different calibers and myringosclerosis, and compare the results with the model of a normal tympano-ossicular chain, previously developed by the authors. The numerical simulations were conducted using the finite element method,[12] which allows simulating mechanical problems, from geometric models, producing results, both in terms of displacements and tensions, for all the constituent components.

2. Materials and Methods

The geometry of the eardrum and ossicles (malleus, incus and stapes) was constructed using computerized tomography images. The images were obtained from a 65 years old woman, without any ear pathology, and the slices have 0.5 mm thickness.[13] Based on this geometry, a finite element mesh was then constructed, including the ligaments, superior, lateral and anterior of the malleus, superior and

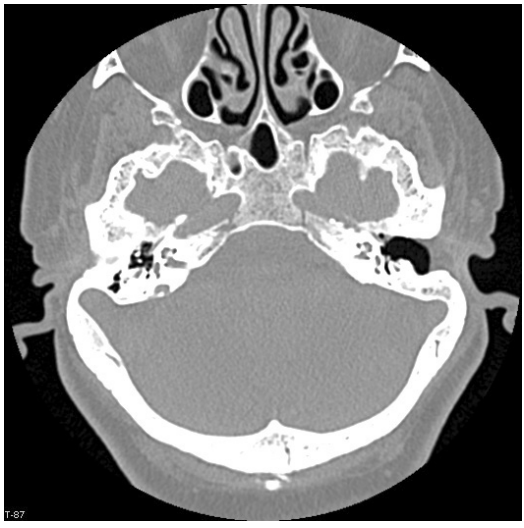

Fig. 2. Sample T-92 CT scan images used with the middle ear and the ossicles.

posterior of the incus, annular ligament of the stapes and two muscles, tensor tympani and stapedius.

Since the CT images obtained from the exams were not suitable for automated segmentation softwares, due to their low resolution, as shown in Fig. 2, a manual procedure was used, using a CAD software.[14,15]

During the image segmentation process, distinguishing the soft tissues constituted a major problem. However, given the anatomy of the middle ear, if the ossicles can be reconstructed and there is enough resolution to perceive the borders of the tympanic cavity, it is possible to use the contour as an accurate estimation of the eardrum dimension. The eardrum, malleus and incus were manually segmented, and 3D geometric solid representations were obtained (Fig. 3).

Due to its reduced dimensions, as shown in Fig. 4, the CT images contained low details on the stapes. Therefore, the stapes was constructed using anatomical bibliographic information.[4] The height and width of the eardrum are respectively 11 mm and 9 mm and its thickness is 0.1 mm, based on Refs. 16–18; the malleus height is 8.5 mm and of the incus, 7 mm; the stapes measures 4.5 mm.

In Fig. 5 the segmentation result for the different ossicles is shown. After this process was completed, the ossicles geometry was imported into a finite element preprocessor, where geometries were reconstructed and prepared for the creation of the finite element mesh.

In order to simulate the cochlear fluid, Abaqus software[19] F3D3 fluid elements were used, assuming an incompressibility condition. Figure 6 shows the geometry constructed for the stapes and the domain used for the fluid, which simulates the cochlear fluid.

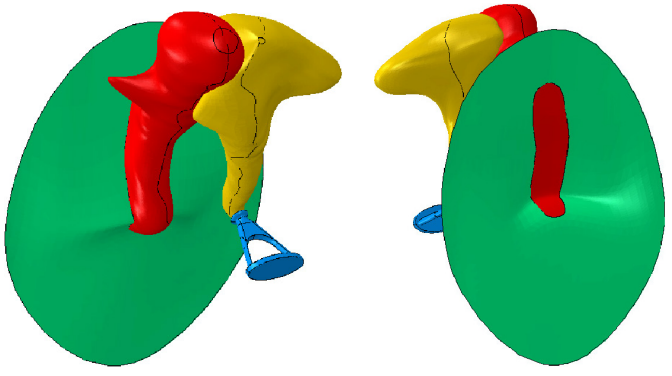

(a) (b)

Fig. 3. (Color online) Three-dimensional representation of the objects: eardrum, malleus, incus and stapes - (a) interior and (b) exterior view, respectively.

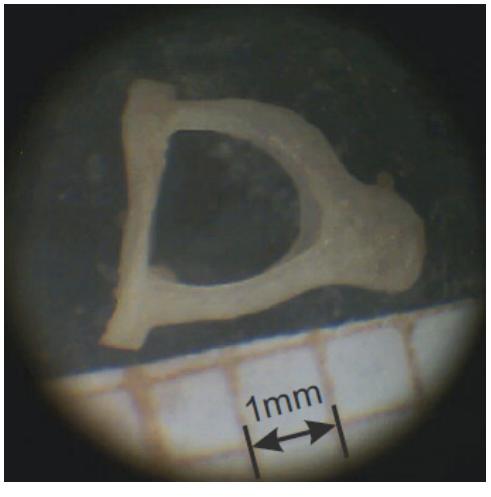

Fig. 4. Photo of a real stapes.

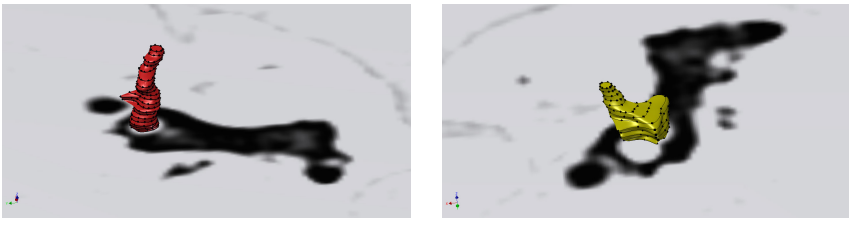

(a) (b)

Fig. 5. (Color online) Ossicles segmentation: (a) malleus; (b) incus.

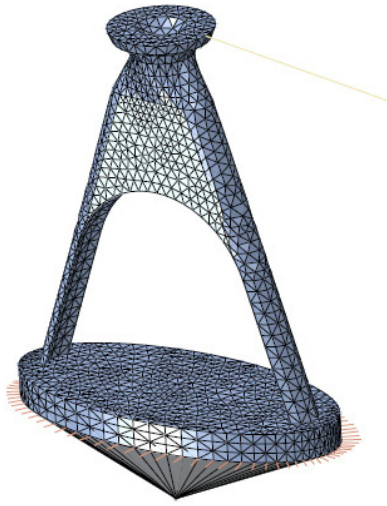

Fig. 6. (Color online) Stapes geometry, stapes annular ligaments and fluid domain.

After all the outlines of the different cross-sections have been obtained, reconstruction was made between them, and finally the 3D geometric model was produced. Using the ABAQUS software,[19] the discretization of the model described was made, starting by the construction of the finite element mesh for the eardrum and then for each of the ossicles. Subsequently, the ossicles were linked and joined with the eardrum, Fig. 7.

The eardrum finite element mesh contains 7648 nodes, with 202 nodes on its periphery, in order to simulate the tympanic sulcus, where the boundary conditions will be applied. The membrane is also formed by 3722 hexahedral elements of type C3D8. From these elements, 302 correspond to the *pars flaccida* and the remaining to the *pars tensa*, Fig. 8.

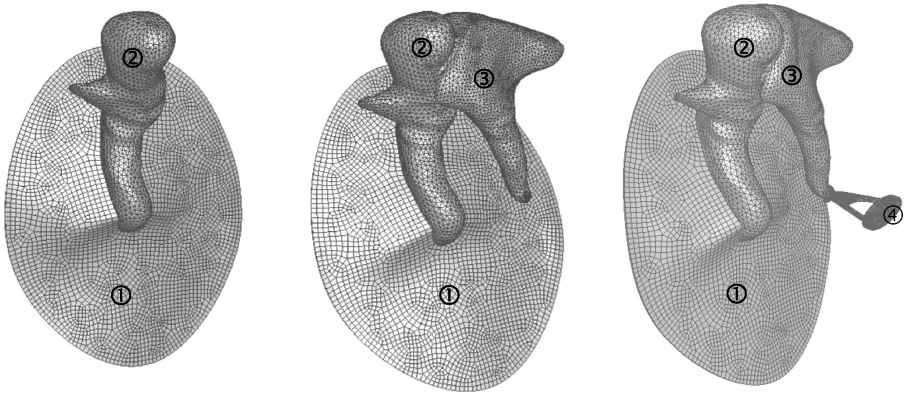

Fig. 7. Finite element mesh of the eardrum ① and ossicles: malleus ②, incus ③ and stapes ④.

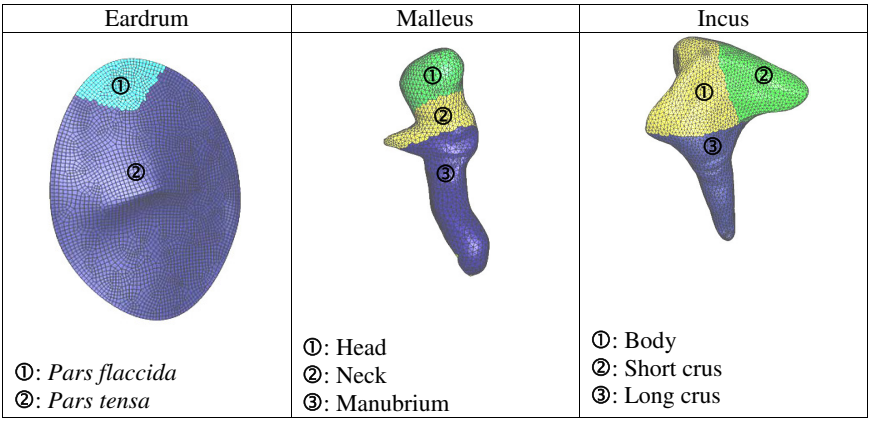

Fig. 8. (Color online) Eardrum, malleus and incus with its division.

All elements relating to the ossicles are tetrahedral C3D4 elements. The mobility of the junction of the malleus with the eardrum depends on the material properties of these elements.

The malleus is formed by 3932 nodes and by 18,841 elements. These elements were divided into three groups: 5163 for the head, 4162 for the neck and 9516 for the manubrium, Fig. 8.

The incus is composed of 8373 nodes and 39,228 elements also distributed into three groups: 16,263 elements for the body, 10,105 for the short crus and 12,860 for the long crus, Fig. 8. The stapes is formed by 2840 nodes and 9218 elements.

The simulation of joints between the ossicles, malleus/incus and incus/stapes was carried out using a mathematical formulation of contact.[20] The contact constraints existing on the joints were modeled using a small sliding contact scheme, with the contact constraints being imposed by Lagrange multipliers, an option available on Abaqus software.[19]

Three ligaments were applied to the malleus (superior, lateral and anterior) and two ligaments to the incus (superior and posterior).

Around the stapes footplate at its periphery, 78 linear elements were placed, formed by the nodes of the footplate and other exterior nodes, simulating the annular ligaments. These ligaments were considered linear elements, with two nodes, of type T3D2. In order to simulate the cochlear fluid, a set of 1056 fluid elements of type F3D3 was created, around the stapes footplate (Fig. 9).

Two muscles (tensor tympani and stapedius) were also included, using linear elements of type T3D2. In total, 22,879 nodes and 72,150 elements were used. In the present work, the ossicles are assumed to have isotropic behavior, with elastic properties summarized in Table 1. The eardrum was divided into *pars flaccida* (with only one layer) and *pars tensa* (with three layers). The *pars flaccida* was considered isotropic with a Young's modulus (E) of $1.00 \times 10^7\ \mathrm{N/m^2}$, like the internal and

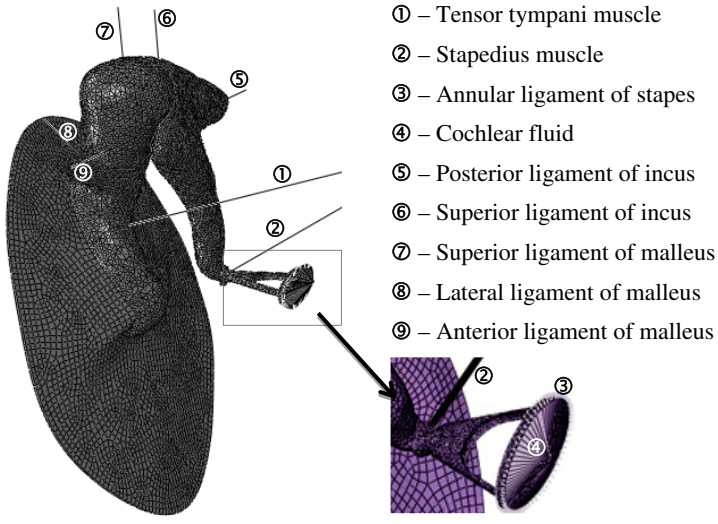

Fig. 9. (Color online) Complete model of tympano-ossicular chain, showing its ligaments, muscles and cochlear fluid.

external layers of the *pars tensa*. The middle layer of the *pars tensa* is modeled as an orthotropic material with tangential Young's modulus (E_q) of $2.00 \times 10^7\,\mathrm{N/m^2}$ and radial Young's modulus (E_r) of $3.20 \times 10^7\,\mathrm{N/m^2}$ (Table 1). The Poisson's ratio (ν) is assumed equal to 0.3 for all materials with $\gamma = 0\,\mathrm{s^{-1}}$ and $\beta = 0.0001\,\mathrm{s}$, as the damping coefficients.[21,22] The malleus and the incus were divided in different areas and the values for their density are shown in Table 1. The stapes take the same

Table 1. Material properties for the eardrum, ossicles and ligaments.

Material properties		Specific mass ($\mathrm{Kg/m^3}$)	Young's modulus ($\mathrm{N/m^2}$)
Eardrum:		1.20×10^3	
	Pars tensa		
	Layer 1		1.00×10^7
	Layer 2		$E_\theta = 2.00 \times 10^7$; $E_r = 3.20 \times 10^7$
	Layer 3		1.00×10^7
	Pars flaccida		1.00×10^7
Ossicles:			1.41×10^{10}
Malleus	– head	2.55×10^3	
	– neck	4.53×10^3	
	– handle	3.70×10^3	
Incus	– body	2.36×10^3	
	– short process	2.26×10^3	
	– long process	5.08×10^3	
Stapes		2.20×10^3	
Ligaments		1.00×10^3	

density value for the whole structure. The value of Young's modulus, for the ossicles, was assumed to be $1.41 \times 10^{10}\,\mathrm{N/m^2}$.

The ligaments and muscles were considered as having an hyperelastic behavior,[23,24] having been used the Yeoh constitutive model,[25] whose material constants[26] are shown in Table 1. The Hill model is a constitutive model adopted in this work, for the middle ear muscles.[27]

The nonlinear theory of elasticity[28] provides the theoretical framework to use the hyperelastic model of Yeoh.[25] The Yeoh model was used to model the mechanical behavior of the ligaments. The Yeoh model has been used successfully by the authors in previous works by Martins *et al.*[26] to study biological materials evidencing a nonlinear elastic behavior associated with large deformations. A detailed description of the model and its application to the middle ear ligaments is presented in Gentil *et al.*[24] The Yeoh model was born as phenomenological approach to study the mechanics of carbon-filled rubbers, which displays a stiffening effect for large strains.[25] Ligaments (in general) also display a nonlinear deformation with a stiffness behavior for large strains. Moreover, the Yeoh model is implemented in commercial finite element solvers such as ABAQUS software[19] and allows for good results using nonlinear optimization algorithms such as Levenberg-Marquardt (LM).[28]

The strain energy function Ψ for the Yeoh model depends only on the first invariant of the right Cauchy–Green strain tensor C[25,29]:

$$\Psi = C_1(I_1^C - 3) + C_2(I_1^C - 3)^2 + C_3(I_1^C - 3)^3,$$
$$I_1^C = \mathrm{tr}\,\mathbf{C} = \mathrm{tr}(\mathbf{F}^T\mathbf{F}).$$

$\mathbf{F}$ being the deformation gradient.

Assuming that the ligament is in a uniaxial stress state, the stretch λ suffered by the ligament, along the sample long axis, will be related with:

$$I_1^C = \lambda_f^2 + \frac{2}{\lambda_f},$$

where λ_f represents the fiber stretch ratio in the direction $\mathbf{N}$ of the undeformed fiber:

$$\lambda_f = \sqrt{\mathbf{N}^T\mathbf{C}\mathbf{N}} = \sqrt{\mathbf{C} : (\mathbf{N} \otimes \mathbf{N})},$$

where $\otimes$ represents the tensor product. The material parameters $\{C_1, C_2, C_3\}$ are the mechanical properties according to the Yeoh model. These parameters must be determined using a numerical optimization scheme adequate for nonlinear problems, such as the LM algorithm.[28]

The experimental data used to estimate the mechanical properties of the middle ear ligaments was published by Wang *et al.*[30] In this work, the authors presented stress-stretch experimental curves from uniaxial tensile tests of the stapedial tendon, the tensor tympani tendon and the anterior malleolar ligament. These curves were fitted using LM algorithm and allowed to establish the material properties

Table 2. Properties for ligaments.

Ligaments/constants		C_1[Pa]	C_2[Pa]	C_3[Pa]
Malleus	– superior	6.3064×10^3	-9.9999×10^3	2.2045×10^6
	– anterior	7.3387×10^4	-3.7438×10^2	5.8557×10^5
	– lateral	6.3064×10^3	-9.9999×10^3	2.2045×10^6
Incus	– superior	6.3064×10^3	-9.9999×10^3	2.2045×10^6
	– posterior	5.4589×10^4	-4.1699×10^4	1.2548×10^6
Stapes	– annular	6.3064×10^2	-9.9999×10^3	2.2045×10^6

according to Yeoh's model $\{C_1, C_2, C_3\}$ assigned to the different ligaments following the suggestions in Wang *et al.*[30] and presented in Table 2.

The constitutive equation adopted in this work for the 3-D passive behavior of the ear muscles is a modified form of the incompressible, transversely isotropic, hyperelastic model proposed by Humphrey and Yin[31] for passive cardiac tissues. The strain energy function, per unit volume of the reference configuration, can be written in the following form:

$$\Psi_{\text{Martins}} = U_I(I_1^C) + U_f(\lambda_f).$$

This strain energy density function is the sum of a term related to the embedding matrix, assumed isotropic and a fiber term. U_I is the strain energy stored in the isotropic matrix embedding the muscle fibers, defined as:

$$U_I = A\{\exp[b(I_1^C - 3)] - 1\}.$$

For the strain energy related with the fiber term U_f, the following expression was used:

$$U_f = A\{\exp[a(\lambda_f - 1)^2] - 1\}.$$

The constitutive parameters used for the muscles are: $c = 1.85 \times 10^{-2}\,\text{N/mm}^2$; $b = 1.173$; $A = 2.80 \times 10^{-2}\,\text{N/mm}^2$ and $a = 0.6215$, according to the work of Martins *et al.*[32]

Since the authors are not aware of any work showing the mechanical properties of an eardrum affected by myringosclerosis, the stiffness of a partial area of the normal eardrum was increased, changing the Young modulus by a factor, in order to simulate the presence of myringosclerosis.

Some studies have shown that myringosclerosis plaques contain calcium and phosphate that form in many cases a Ca/P ratio close to hydroxyapatite.[33–37] The article of Ching *et al.*[35] suggest a value for the Young modulus of $120.6 \times 10^9\,\text{N/m}^2$. In the present work a study based on the original value of the eardrum was done and the influence of the Young modulus was analyzed for distinct increased factors: 10, 50 and 10,000 (the last one is based on the work of Ching *et al.*[35]). This study allowed to conclude that the stapes displacements are no different for values of the

multiplicative factor greater than 10, so the value used for the Young modulus of plaques was $1.0 \times 10^8\,\mathrm{N/m^2}$ (which means an increased factor of 10).

The set formed by the three ossicles is fixed in its outer portions to the eardrum by the malleus and inside by the oval window, through the stapes. The ossicles are still suspended by ligaments and muscles.

Boundaries of the finite element model include the *pars tensa* of the eardrum periphery simulating the tympanic sulcus; the connection between the stapes footplate and the cochlea, in the oval window, simulating the stapes annular ligament, where the free extremities of these elements are fixed, while the others are connected to the stapes nodes; the superior ligament of the malleus is attached to the head of the malleus and the superior ligament of the incus is attached to the incus body, with opposing nodes fixed, simulating the fixation to the upper wall of the tympanic cavity; the lateral ligament of the malleus is attached to the tympanic sulcus and the opposing node is attached to the neck of the malleus; the anterior ligament of malleus is attached to the neck of the malleus, with the opposing node fixed in a previous plane, simulating the anterior wall of the tympanic cavity; the posterior ligament of the incus is attached to the short crus, with the opposing node being fixed in a plane that simulates the posterior wall of tympanic cavity; the tensor tympanic muscle is attached to the upper end of the manubrium of the malleus and the stapedius muscle is attached to the head of the stapes, near posterior crura, with the opposing nodes being fixed.

With the aim of understanding the behavior of the tympano-ossicular chain, for frequencies ranging between 100 Hz and 10 kHz (the most important audible range), several studies were made based on dynamic analyses, with a pressure of 2 Pa applied in the eardrum (equivalent to 100 dB SPL).

The first simulation was made in order to compare the behavior of a normal ear with the behavior of an ear that has been perforated with three different calibers[38] (0.6, 2.0 and 7.0 mm), Fig. 10.

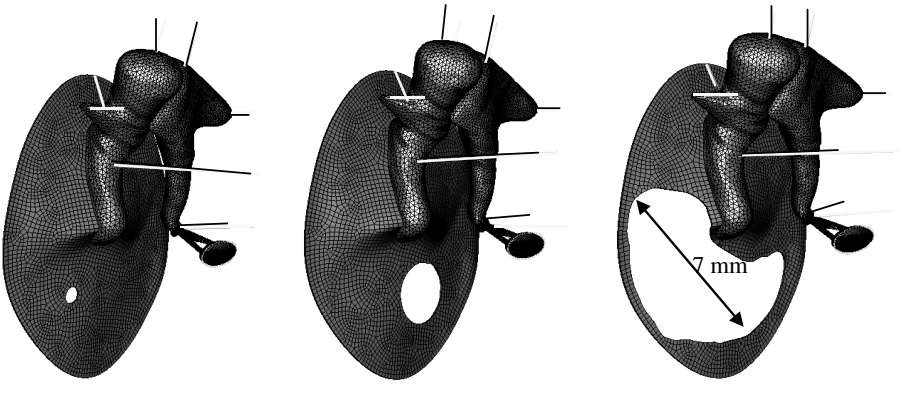

Fig. 10. Three eardrum perforations of different calibers of diameter, respectively (0.6 mm; 2 mm and 7 mm).

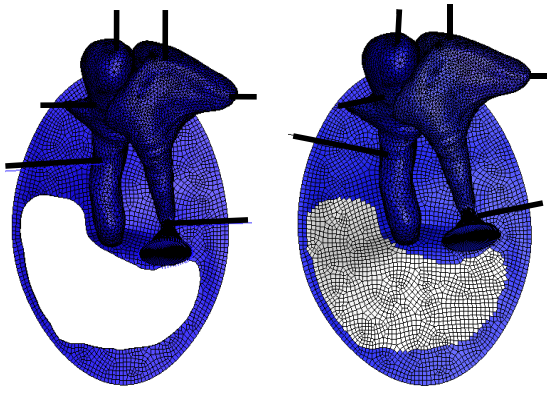

(a) (b)

Fig. 11. (Color online) (a) Perforation of 7 mm; (b) Equal area covered by myringosclerosis.

Next, a simulation to study the effect of different areas of the *pars tensa* covered by myringosclerosis was made. Two comparisons were made: the behavior of an ear that has been perforated with a caliber of 7.0 mm with the same ear but with the area that was previously removed, now being covered by myringosclerosis, Fig. 11.

The second comparison was between an ear with a perforation of 2.0 mm with the same ear but now with the remaining eardrum covered with myringosclerosis, Fig. 12.

The results were obtained with respect to the umbo displacement (the central part of the eardrum) and the central part of the stapes footplate. The model without

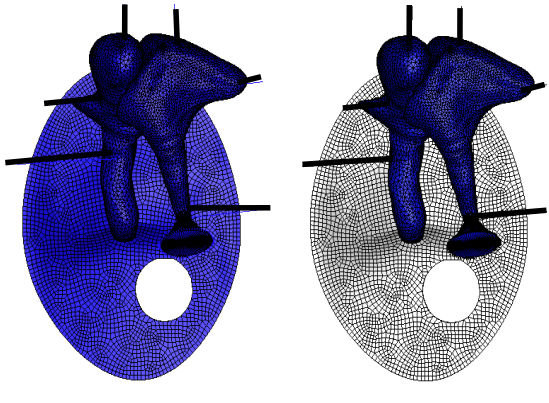

(a) (b)

Fig. 12. (Color online) (a) Perforation of 2 mm of diameter with the remainder eardrum normal. (b) Perforation of 2 mm of diameter and remainder eardrum with myringosclerosis.

any modification, considered normal, was used to compare the results obtained from the following numerical simulations:

- A numerical simulation to access the effect of three different sizes of perforations (diameters of 0.6, 2.0 and 7.0 mm).
- A numerical simulation to verify the differences between an eardrum with a perforation of 7.0 mm in diameter with another eardrum where the perforation is now covered by myringosclerosis.
- A numerical simulation to compare an eardrum with a perforation of 2.0 mm, maintaining the remaining eardrum normal, with another simulation, that maintain the 2.0 mm perforation and the remaining eardrum was affected by myringosclerosis.

3. Results and Discussion

In order to validate the model created for the normal ear, a dynamic study was made for a frequency range between 100 Hz and 10 kHz. A sound pressure of 0.2 Pa and 3.557 Pa was applied in the eardrum, which correspond respectively to 80 dB SPL and 105 dB SPL. For 80 dB SPL the results were compared with the results obtained by Lee *et al.*[39] and Prendergast *et al.*[21] It should be noted that the Lee's study is experimental and that the Prendergast is computational. For 105 dB SPL, the results were compared with the experimental study of Kurokawa.[40] Figure 13 shows the stapes footplate displacement, which are in accordance with the results obtained by the different authors.

It must be noted that displacements referred in all figures correspond to peak amplitude and that stapes displacements are general motion.

The displacements for a node belonging to the umbo, for the normal ear and for a perforated ear with three perforations of different sizes (0.6, 2.0 and 7.0 mm) are shown in Fig. 14. In Fig. 15, the displacements for the central part of the stapes footplate are shown.

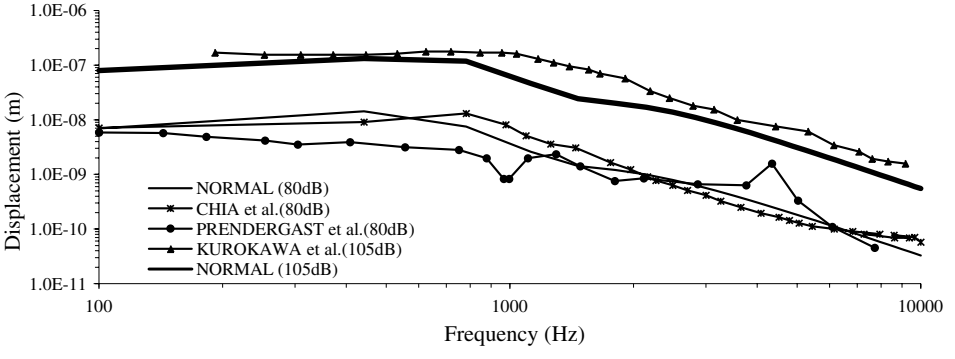

Fig. 13. Stapes footplate displacement for 80 and 105 dB SPL applied in the eardrum. Comparison of the obtained results (normal) with reference works.

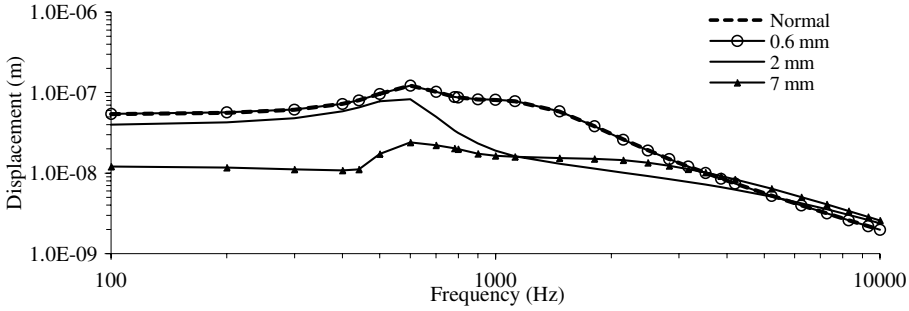

Fig. 14. Umbo displacement, comparing the normal ear with three eardrum perforations.

It can be concluded that the microperforation (0.6 mm) does not display differences in displacements neither in the umbo nor in the central part of the stapes footplate, when compared with the normal eardrum. Concerning the perforation of 2.0 mm, there are also no significant differences in the umbo displacement, in low and high frequencies, showing a smaller displacement at the level of medium frequencies (Fig. 14). For the perforation of 2.0 mm, there is no significant difference between the stapes displacements (Fig. 15). The larger differences occur in the perforation of 7.0 mm, showing smaller displacements, both for the umbo, and for the central part of the stapes footplate, especially in the lower and middle frequencies. In all cases, for high frequencies there were no significant differences in displacements.

The effect of eardrum perforations on sound transmission through the middle ear has been investigated by other authors, and the outcome of this study is in agreement with those results, taking into consideration that there is a linear relationship between the increasing size of a perforation and the conductive hearing loss.[41] Moreover, the perforation-induced losses are greatest at the lowest frequencies, as larger perforations result in larger hearing losses.[10] The conductive hearing loss resulting from a tympanic membrane perforation is frequency-dependent, with the largest losses occurring at the lowest sound frequencies. The conductive hearing loss increases as the size of the perforation increases.[7]

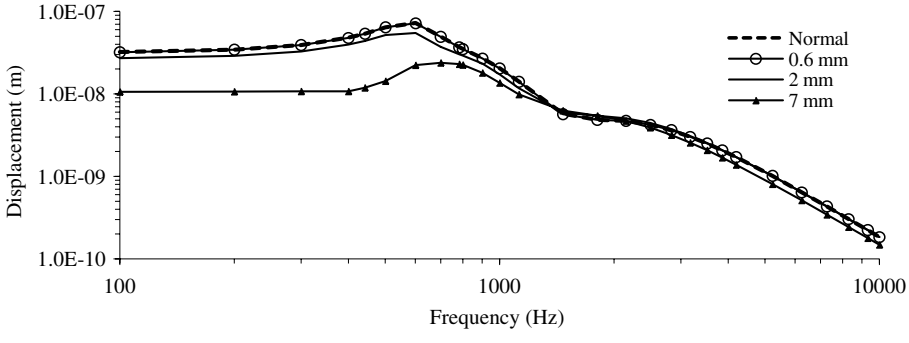

Fig. 15. Stapes footplate displacements, comparing the normal ear with the three eardrum perforations.

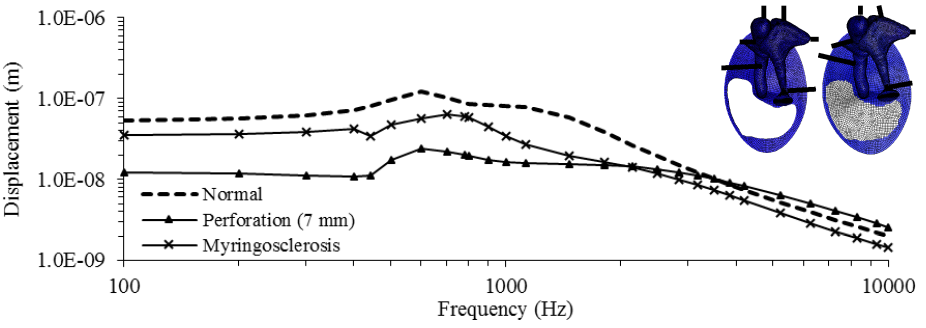

Fig. 16. Umbo displacement comparing the normal ear with 7 mm eardrum perforation and equal area covered by myringosclerosis.

The work reported by Gan[6] showed that the perforation of eardrum mainly affected the umbo and stapes displacement at low frequency range (below 2 kHz), even the size of the hole is very small. The difference between the obtained results and the reference cited may be related to the absence of the tympanic cavity in the model proposed where only the tympano-ossicular chain is considered.

In the clinical practice, the Electrocochleography (ECochG), which is a technique of recording of electrical potentials of the inner ear using an invasive method with electrodes like transtympanic needle, causes a microperforation (more or less 0.6 mm of diameter). However, this practice does not induce any hearing loss.

In this paper, the smaller perforation (0.6 mm in diameter) corresponds to 0.5% of total eardrum area, and the second one to 5% (2 mm in diameter). Comparing the results of the present work with the results published by Lerut *et al.*,[41] one can check that the air bone gap for perforations with this range of dimensions present values around 10 dB, which are close to the normal hearing.

In the second simulation, the comparison between the models of an ear with a perforation of 7.0 mm and the same perforated ear with the removed area covered by myringosclerosis was made. Figure 16 shows the differences between their respective displacements obtained at the umbo. Throughout the frequency range, the displacements are smaller in the case of the perforated ear for low and middle frequencies, showing no differences for high frequencies.

When one considers the same area hit by myringosclerosis, results are closer to the normal ear for low and middle frequencies. No differences were obtained again for higher frequencies. The same results were obtained when comparing the displacements of the central part of the stapes footplate, Fig. 17.

It should be noted that the results obtained in the model with myringosclerosis are very similar to normal ear. The biggest differences (smaller displacements) have been found in low frequencies. In the case of a perforation with a caliber of 7.0 mm, no significant differences were obtained for high frequencies. These results are in

accordance with the clinical practice, which points to hearing losses more pronounced in cases of perforations with this magnitude and for low frequencies. The clinical practice also point to patients not evidencing significant hearing loss in cases where the myringosclerosis appears individually.

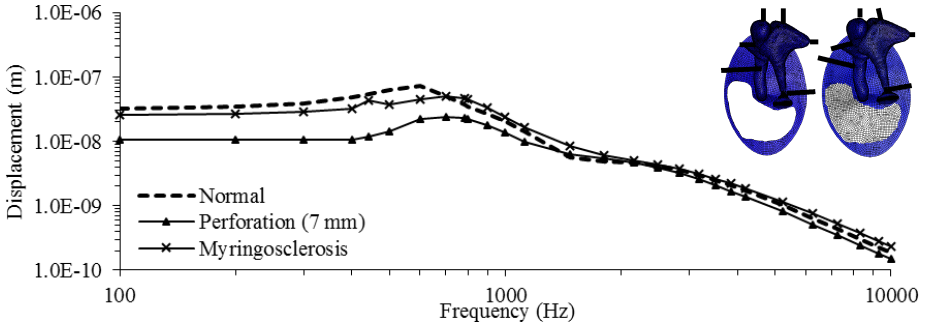

Fig. 17. Stapes footplate displacement, comparing normal ear with 7 mm eardrum perforation and equal area covered by myringosclerosis.

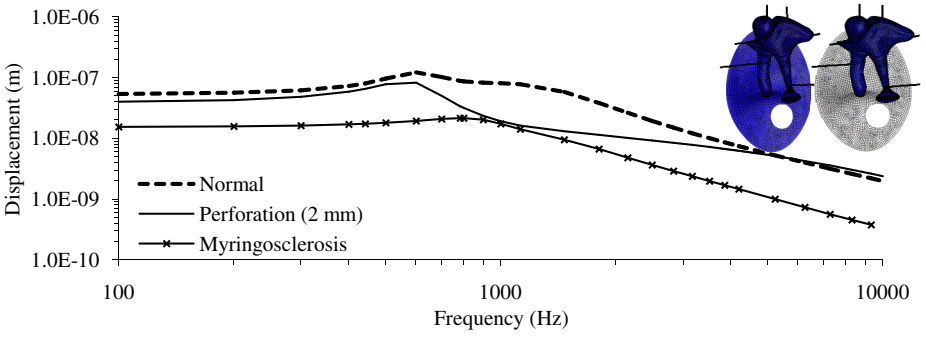

Fig. 18. Umbo displacement, comparing the normal ear with the 2 mm eardrum perforation, with the remaining area of the eardrum normal or covered by myringosclerosis.

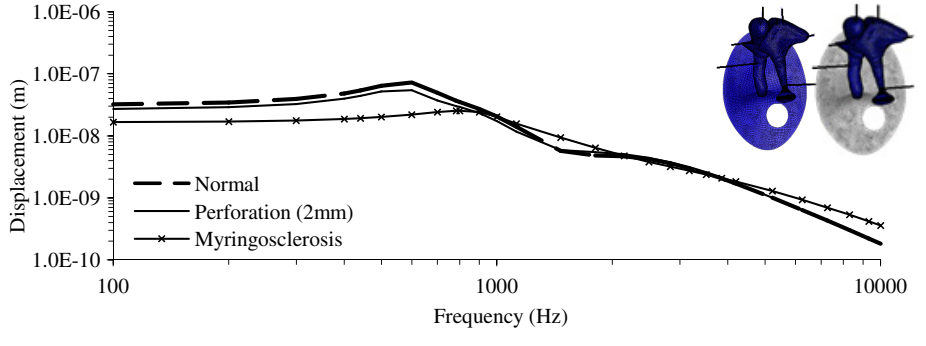

Fig. 19. Stapes footplate displacements, comparing the normal ear with the 2 mm perforation, with the remaining area of the eardrum normal or covered by myringosclerosis.

The audiometric repercussion is scarce if only myringosclerosis occurs, with possible transmission hearing loss if malleus or other ossicles are involved.[42,43]

Figures 18 and 19 show the results for the simulation of a 2.0 mm perforation, with the remaining normal eardrum and the same perforation with the remaining eardrum hit by myringosclerosis. These results were also compared with the model representative of a normal ear. In this case, since the perforation is smaller, the results are more approximate to those of normal hearing. However, when the perforation is associated with myringosclerosis on the remaining eardrum, there is a decrease in the displacements, in particular in the stapes footplate, which might be related with greater hearing losses.

4. Conclusions

After the results were obtained for the three perforations, it can be concluded that the microperforation (0.6 mm) presents no differences in terms of the displacement of the umbo or the central part of stapes footplate, when compared with the normal eardrum. Concerning the perforation of 2.0 mm there is only a little difference at middle frequencies for the umbo displacement, showing a slight decrease in the displacements in the central part of stapes footplate. The largest differences occur with a perforation of 7.0 mm, showing smaller displacements in low and middle frequencies, both for the umbo and stapes footplate, which is related with major hearing loss in this frequency range. In all cases, for high frequencies there are no differences in displacements.

With regard to myringosclerosis, it was found that there are major differences (smaller displacements) in the umbo than in the central part of the stapes footplate, i.e., the eardrum vibrates less with the increased stiffness due to myringosclerosis presence. However, regarding the stapes footplate, there are no significant differences when compared with the normal ear, which agrees with the clinical data, which refers that myringosclerosis does not cause large hearing losses when this pathology appears isolated. Regarding the eardrum, this decrease of displacement only relates to the higher stiffness caused by myringosclerosis and is not directly associated with hearing losses. When, there is an eardrum perforation along with myringosclerosis, the displacements decrease, both in the umbo and in the central part of the stapes footplate, often associated with a pronounced hearing loss.

One limitation of this work is the absence of the tympanic cavity, with only the tympano-ossicular system being considered in the model, which can explain differences with some published works. Therefore, studies with tympanic cavity would be required to ensure appropriate generalization of the findings of the study.

It is known that if only a small increment of the stiffness of eardrum occurs, it will have no repercussion in terms of hearing loss. Myringosclerosis is more common and only rarely associated with hearing loss. Thus, it can be concluded that reduced displacement in the stapes footplate may be related with greater hearing losses.

Acknowledgments

The authors would like to thank the Ministério da Ciência, Tecnologia e Ensino Superior — Fundação para a Ciência e a Tecnologia in Portugal and by FEDER for the funding provided under the research project "Estudo bio-computacional do zumbido" with the reference PTDC/SAU-BEB/104992/2008, and research grant SFRH/BPD/1080/2010, and SFRH/BD/74731/2010.

References

1. Isaacson JE, Vora NM, Differential diagnosis and treatment of hearing loss, *Am Acad Fam Physicians* **68**:1125–1132, 2003.
2. Mirko T, *Manual of Middle Ear Surgery: Surgical Solutions for Conductive Hearing Loss*, Thieme, New York, 2000.
3. Paço J, *Doenças do Tímpano*, Lidel, Lisboa, 2003.
4. Sanna M, Russo A, Donato GD, *Color Atlas of Otoscopy – From Diagnosis to Surgery*, Thieme Stuttgart, New York, 1999.
5. Bigelow DC, Swanson PB, Saunders JC, The effect of tympanic membrane perforation size on umbo velocity in the rat, *Laryngoscope* **106**:71–76, 1996.
6. Gan RZ, Cheng T, Dai C, Yang F, Wood MW, Finite element modeling of sound transmission with perforations of tympanic membrane, *J Acoust Soc Am* **126**:243–253, 2009.
7. Mehta RP, Rosowski JJ, Voss SE, O'Neil E, Merchant SN, Determinants of hearing loss in perforations of the tympanic membrane, *Otol Neurotol* **27**:136–143, 2006.
8. Voss SE, Rosowski JJ, Merchant SN, Peake WT, Middle-ear function with tympanic-membrane perforations. I. Measurements and mechanisms, *J Acoust Soc Am* **110**:1432–1444, 2001.
9. Voss SE, Rosowski JJ, Merchant SN, Peake WT, Middle-ear function with tympanic-membrane perforations. II. A simple model, *J Acoust Soc Am* **110**:1445–1452, 2001.
10. Voss SE, Rosowski JJ, Merchant SN, Peake WT, How do tympanic-membrane perforations affect human middle-ear sound transmission? *Acta Otolaryngol.* **121**:169–173, 2001.
11. Voss SE, Rosowski JJ, Merchant SN, Peake WT, Non-ossicular signal transmission in human middle ears: Experimental assessment of the "acoustic route" with perforated tympanic membranes, *J Acoust Soc Am* **122**:2135–2153, 2007.
12. Ferreira AJM, Elementos finitos em Matlab, 2007.
13. Gentil F, Jorge RN, Parente MPL, Martins PALS, Ferreira AJM, Estudo biomecânico do ouvido médio, *Clínica e Investigação em Otorrinolaringologia* **3**(1):24–30, 2009.
14. Alexandre F, Fernandes AA, Jorge RN, Gentil F, Martins P, Mascarenhas T, Milheiro C, Ferreira AJM, Parente MPL, 3D reconstruction of the middle ear for FEM simulation, in Tavares JMRS, Natal Jorge RM (eds.), *Simpósio Internacional CompIMAGE - Computational Modelling of Objects Represented in Images: Fundamentals, Methods and Applications*, Coimbra, pp. 181–184, 2006.
15. Alexandre F, Jorge RN, Tavares JM, Mascarenhas T, El Sayed RF, Fernandes AA, Gentil F, Ferreira AJM, Segmentação e reconstrução 3D de estruturas em imagens médicas: Comparação entre uma metodologia automática e uma outra manual, CMNE/CILAMCE, Porto, 2007.
16. Gan RZ, Feng B, Sun Q, Three-dimensional finite element modeling of human ear for sound transmission, *Ann Biomed Eng* **32**(6):847–859, 2004.

17. Koike T, Wada H, Kobayashi T, Modeling of the human middle ear using the finite element method, *J Acoust Soc Am* **3**:1306–1317, 2002.
18. Wever EG, Lawrence M, *Physiological Acoustics*, Princeton University Press, 1982.
19. Hibbit D, Karlsson B, Sorenson P, *ABAQUS Analysis User's Manual*, version 6.5, Hibbit, Karlsson & Sorenson Inc., USA, 2004.
20. Gentil F, Natal Jorge RM, Ferreira AJM, Parente MPL, Moreira M, Almeida E, Estudo do efeito do atrito no contacto entre os ossículos do ouvido médio, *Rev Int Métod Numér Cálc Diseñ Ing* **23**:177–187, 2007.
21. Prendergast PJ, Ferris P, Rice HJ, Blayney AW, Vibro-acoustic modelling of the outer and middle ear using the finite-element method, *Audiol Neuro-Otol* **4**:185–191, 1999.
22. Sun Q, Gan RZ, Chang KH, Dormer KJ, Computer-integrated finite element modeling of human middle ear, *Biomech Model Mechanobiol* **1**:109–122, 2002.
23. Gentil F, Jorge RMN, Ferreira AJM, Parente MPL, Martins PALS, Almeida E, Biomechanical simulation of middle ear using hyperelastic models, *J Biomech* **39**(1):388–389, 2006.
24. Gentil F, Parente M, Martins P, Garbe C, Jorge R, Ferreira A, Tavares J, The influence of mechanical behaviour of the middle ear ligaments: A finite element analysis, *J Eng Medi*, **225**(1): 68–76, 2011.
25. Yeoh OH, Characterization of elastic properties of carbon-black-filled rubber vulcanizates, *Rubber Chem Technol*, **63**:792–805, 1990.
26. Martins PALS, Jorge RMN, Ferreira AJM, A comparative study of several material models for prediction of hyperelastic properties: Application to silicone-rubber and soft tissues, *Strain* **42**:135–147, 2006.
27. Gentil F, Parente M, Martins P, Garbe C, Paço J, Ferreira AJM, Tavares JMRS, Jorge RN, The influence of muscles activation on the dynamical behaviour of the tympano-ossicular system of the middle ear, *Comput Method Biomech Biomed Eng*, doi: 10.1080/10255842.2011. 623674.
28. Marquardt DW, An algorithm for least-squares estimation of nonlinear parameters, *SIAM J Appl Math* **11**:431–441, 1963.
29. Holzapfel GA, *Nonlinear Solid Mechanics*, Wiley, New York, 2000.
30. Wang X, Cheng T, Gan R, Finite-element analysis of middle-ear pressure e effects on static and dynamic behavior of human ear, *J Acoust Soc Am* **122**:906–917, 2007.
31. Humphrey JD, Yin FCP, On constitutive relations and finite deformation of passive cardiac tissue: A pseudostrain-energy function, *J Biomech Eng* **109**:298–304, 1987.
32. Martins J, Pires E, Salvado R, Dinis P, A numerical model of passive and active behavior of skeletal muscles, *Comput Methods Appl Mech Eng* **151**:419–433, 1998.
33. Buyanover D, Tietz A, Luntz M, Sad J, The biochemical composition of tympanosclerotic deposits, *Archi Otorhinolaryngol* **243**:366–369, 1987.
34. Chang IW, Tympanosclerosis, Electron microscopic study, *Acta Otolaryngol* **68**:62–72, 1969.
35. Ching WY, Rulis P, Misra A, Ab initio elastic properties and tensile strength of crystalline hydroxyapatite, *Acta Biomater* **5**:3067–3075, 2009.
36. Doner F, Yariktas M, Dogru H, Uzun H, Aydin S, Delibas N, The biochemical analysis of tympanosclerotic plaques, *Otolaryngol Head Neck Surg* **128**(5):742–745, 2003.
37. Gibb AG, Pang YT, Current considerations in the etiology and diagnosis of tympanosclerosis, *Eur Arch Oto-Rhino-Laryngol* **251**:439–451, 1994.
38. Gentil F, Natal Jorge RM, Ferreira AJM, Parente MPL, Martins PALS, Almeida E, A static and dynamic study of the middle ear with different sizes of eardrum perforations, in *8th Int Symp Comp Methods in Biomechanics and Biomedical Engineering, CMBBE*, Porto, 2008.
39. Lee CF, Chen PR, Lee WJ, Chen JH, Liu TC, Computer aided three-dimensional reconstruction and modeling of middle ear biomechanics by high-resolution computed tomography and finite element analysis, *Biomed Eng-Appl Basis Commun* **18**(5) 214–221, 2006.
40. Kurokawa H, Goode RL, Sound pressure gain produced by the human middle ear, *Otolaryngol Head Neck Surg* **113**(4):349–355, 1995.
41. Lerut B, Pfammatter A, Moons J, Linder T, Functional correlations of tympanic membrane perforation size, *Otol Neurotol* **33**:379–386, 2012.
42. Risueño MT, *Atlas de Otoscopia*, Revisfarma, Edições Médicas, Lda, Madrid, 2006.
43. Roland PS, Marple BF, Meyerhoff WL, *Hearing Loss*, Thieme, New York, 1997.